AD-A060 741 NAVAL RESEARCH LAB WASHINGTON D C F/G 11/6
EFFECT OF HEAT TREATMENT ON FATIGUE CRACK PROPAGATION AND DEFOR--ETC(U)
JUL 78 H H SMITH, D J MICHEL
UNCLASSIFIED NRL-MR-3810 SBIE-AD-E000 212 NL

| OF |
AD
A060741

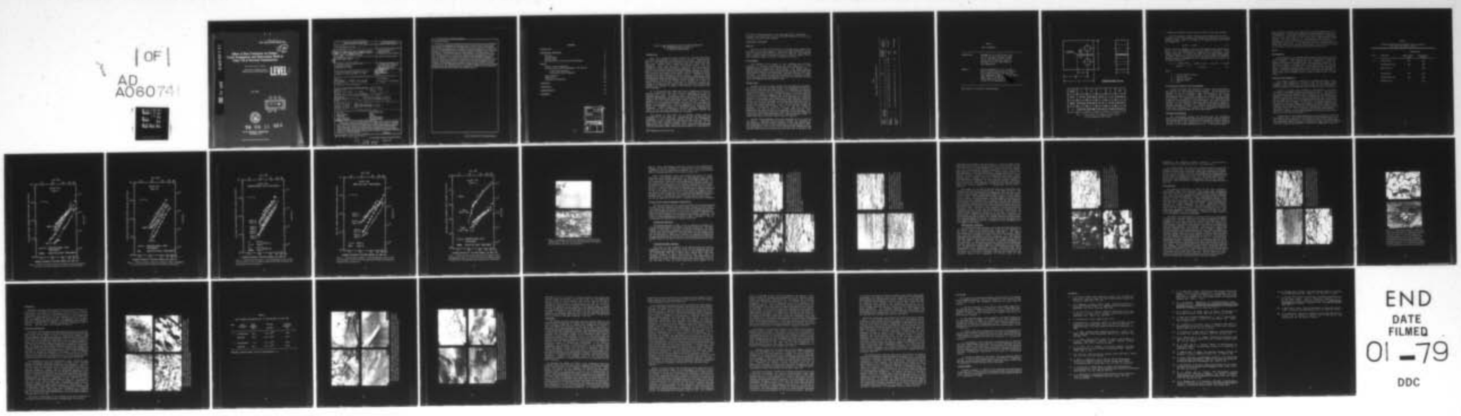

END
DATE
FILMED
01-79
DDC

ade 000212

NRL Memorandum Report 3810

12 DW

Effect of Heat Treatment on Fatigue Crack Propagation and Deformation Mode in Alloy 718 at Elevated Temperatures

H. H. SMITH AND D. J. MICHEL

Thermostructural Materials Branch
Material Science and Technology Division

LEVEL II

July 1978

78 09 11 023

NAVAL RESEARCH LABORATORY
Washington, D.C.

SECURITY CLASSIFICATION OF THIS PAGE (When Data Entered)

REPORT DOCUMENTATION PAGE

READ INSTRUCTIONS BEFORE COMPLETING FORM

1. REPORT NUMBER NRL Memorandum Report 3810	2. GOVT ACCESSION NO.	3. RECIPIENT'S CATALOG NUMBER
4. TITLE (and Subtitle) 6 EFFECT OF HEAT TREATMENT ON FATIGUE CRACK PROPAGATION AND DEFORMATION MODE IN ALLOY 718 AT ELEVATED TEMPERATURES.		5. TYPE OF REPORT & PERIOD COVERED Interim topical report on a continuing problem. 6. PERFORMING ORG. REPORT NUMBER
7. AUTHOR(s) 10 H.H. Smith ~~and~~ D.J. Michel		8. CONTRACT OR GRANT NUMBER(s)
9. PERFORMING ORGANIZATION NAME AND ADDRESS Naval Research Laboratory Washington, D.C. 20375		10. PROGRAM ELEMENT, PROJECT, TASK AREA & WORK UNIT NUMBERS NRL Problem M01-14 & M01-27 Project EX-76A-27-2110 & ~~RR02-11-41-5426~~ 022 11-41
11. CONTROLLING OFFICE NAME AND ADDRESS Office of Naval Research, Arlington, VA 22217 and Department of Energy, Washington, D.C. 20545		12. REPORT DATE 11 July 1978 13. NUMBER OF PAGES 38
14. MONITORING AGENCY NAME & ADDRESS (if different from Controlling Office) 14 NRL-MR-381Ø		15. SECURITY CLASS. (of this report) UNCLASSIFIED 15a. DECLASSIFICATION/DOWNGRADING SCHEDULE

16. DISTRIBUTION STATEMENT (of this Report)

Approved for public release; distribution unlimited.

9 Interim rept., 12 39p.

17. DISTRIBUTION STATEMENT (of the abstract entered in Block 20, if different from Report)

16 RRØ2211 / 17 RRØ221141

18. SUPPLEMENTARY NOTES

18 SBIE 19 AD-EØØØ 242 61153N

19. KEY WORDS (Continue on reverse side if necessary and identify by block number)

Alloy 718	Environmental effects
Crack propagation	Fatigue
Deformation	Hold time
Electron microscopy	Mechanical properties
Elevated temperatures	Precipitate formation

20. ABSTRACT (Continue on reverse side if necessary and identify by block number)

Alloy 718 is a commercial, wrought nickel-base alloy widely utilized in moderate temperature structural applications and has been proporsed for use in advanced nuclear systems. In such applications, Alloy 718 will experience the combined effects of cyclic and static loading and sustained elevated temperatures. However, when used in structures requiring welds, Alloy 718 exhibits reduced weld ductility and strain age cracking when given conventional post-weld duplex age heat treatments. A modified heat treatment has been previously proposed to obviate these problems and thereby improve structural reliability.

(Continues)

DD FORM 1473 1 JAN 73 EDITION OF 1 NOV 65 IS OBSOLETE i

S/N 0102-014-6601

SECURITY CLASSIFICATION OF THIS PAGE (When Data Entered)

78 09 11 023

251 950

20. Abstract (Continued)

The effect of conventional and modified heat treatments and combined cyclic and static loading (hold time) on crack propagation and deformation mode in two heats of Alloy 718 plate material was investigated at 427 and 593 deg C. The fatigue results show that, in general, the resistance of Alloy 718 to crack propagation at these temperatures was not adversely affected by the modified heat treatment and, under most conditions, was found to be improved in comparison with the conventional heat treatment. Scanning electron microscopy (SEM) examination of the fracture surfaces of the fatigue specimens revealed that the failure mode was dependent on test temperature and heat treatment. The material given the conventional heat treatment exhibited transgranular failure modes at both test temperatures. On the other hand, the modified heat treatment produced transgranular fractures at 427 deg C and intergranular or a mixed failure mode at 593 deg C. Transmission electron microscopy (TEM) techniques were used to characterize the microstructure produced by both heat treatments. The relationships between microstructure, failure mode, and deformation mechanisms contributing to the crack propagation behavior were investigated using plane strain specimens deformed in plastic bending. The results are discussed on the basis of the comparison between the plane strain deformation mechanisms and the observed crack propagation behavior.

CONTENTS

INTRODUCTION 1

EXPERIMENTAL PROCEDURES 2

- Material 2
- Microhardness 2
- Fatigue Tests 2
- Microstructural Analysis and Fractography 6

RESULTS 7

- Fatigue Crack Propagation 7
- Microstructural and Fractographic Ovservations 14
  - As-Received Condition 14
  - Conventional Heat Treatment 14
- Phase Analysis 20
- TEM Results 23
- Deformation Mechanisms 23

DISCUSSION 28

CONCLUSIONS 32

ACKNOWLEDGMENTS 32

REFERENCES 33

EFFECT OF HEAT TREATMENT ON FATIGUE CRACK PROPAGATION AND DEFORMATION MODE IN ALLOY 718 AT ELEVATED TEMPERATURES

INTRODUCTION

Alloy 718 is presently being considered for elevated temperature structural applications in breeder reactor systems. However, recent work (1) has shown that Alloy 718 may exhibit low weld ductility and heat treat cracking after conventional post-weld duplex age heat treatments. Alloy 718 and other nickel-base alloys (2,3) are susceptible to heat treat cracking as a result of a critical reduction in ductility within the heat treating temperature range of the alloys. When in this brittle condition, residual welding stresses or thermal cycle stresses may produce strains which cannot be accommodated by the microstructure and cracking or failure occurs. Because of these problems of low ductility and heat treat cracking in conventionally heat treated welds, severe design penalties are being imposed on welded Alloy 718 components proposed for breeder reactor systems. As a result of studies by Keiser (1) which identified the conditions, causes, and methods for preventing heat treat cracking in Alloy 718, a modified heat treatment was proposed to improve weld ductility and minimize heat treat cracking.

It is recognized that under the service conditions of breeder reactor systems the Alloy 718 structural components will have to withstand the effects of static, cyclic, and combined loading at elevated temperatures. Studies have been conducted to determine the effect of the modified heat treatment on tensile properties (1), impact strength (4), and crack growth under static load (5) of Alloy 718. James (6,7) has extensively studied the effect of heat treatment on fatigue crack propagation at elevated temperatures in Alloy 718 base metal and weldments given the conventional and modified heat treatments. Little information is available, however, regarding the effect of the two heat treatments on the relationship between the microstructure and deformation behavior in fatigue.

The purpose of this report is to present results from an investigation of the effect of conventional and the modified heat treatments on the relationship between fatigue crack propagation performance, fracture modes and microstructure of Alloy 718. To meet these objectives, selected fatigue tests were conducted at two temperatures and loading conditions and an extensive metallographic study was performed. These results were then applied to a discussion of

Note: Manuscript submitted June 26, 1978.

the effect of microstructure on the high temperature deformation processes and failure modes in Alloy 718 when subjected to cyclic and combined cyclic and static loading.

EXPERIMENTAL PROCEDURES

Material

Two heats of Alloy 718 received in the wrought plate product form were used in this investigation. Both alloys were produced by vacuum induction melting and refined by vacuum arc remelting. The material sources and the chemical analyses are given in Table 1. Details of the heat treatments given the alloys are presented in Table 2.

Microhardness

The response of the alloys to heat treatment was initially evaluated by hardness measurements at room temperature. The measurements were performed on a microhardness tester using a 136° diamond pyramid indentor and 100 gm weight. The diamond pyramid microhardness (DPH) data reported represent the average of at least five determinations taken from unstressed, polished portions of tested specimens. In instances where the microstructure indicated possible acute inhomogeneities, microhardness data were also obtained in these areas and compared with the general value.

Fatigue Tests

Standard 1/2T and 1T compact tension (CT) specimens meeting ASTM E-399 criteria were used for the fatigue crack propagation evaluations. The specimen dimensions are shown in Fig. 1. All specimens were machined from plate material in the L-T orientation (i.e., the fracture plane was normal to the length or final rolling direction of the plate and the direction of fracture propagation was coincident with the transverse direction of the plate). Crack growth in the specimens was monitored remotely on one specimen side surface using a high resolution television system. In the 1/2T CT specimen, crack length determinations proved to be difficult because the crack was very straight and sharp with no visible associated deformation. The 1/2T CT specimen design was modified to incorporate a deeper notch, 13.7 mm, and a longer W dimension, 34.3 mm, to allow for a longer crack run but still maintaining a/W ratios similar to the standard 1/2T CT specimens. This modification essentially provided a longer crack length and appeared to facilitate crack length measurement by allowing a greater number of length samplings particularly when failure was imminent.

Fatigue crack propagation tests were performed in air at 427 and 593 deg C. Sawtooth, zero-to-tension loading was performed in electrohydaulic testing machines operating in the load control mode. The stress ratio, R (i.e., ratio of minimum to maximum applied stress), was approximately 0.05 for all tests. Specimen test temperature was achieved inductively and temperatures were controlled to ±3 deg C with

Table 1

Chemical Composition of Specimen Materials

Heat No. and Producer	NRL Heat Designation	C	Mn	P	S	Si	Cr	Ni	Ti	Al	Mo	Nb & Ta	Co	Cu	B	Fe	Melting and Remelting Procedures	As-Received Condition
02AOES Huntington	A	.02	.10	.02	.007	.18	18.27	53.29	1.01	.54	3.07	5.10	.06	.04	.003	18.30	IVM: VAR	Hot Rolled
2180-2-9251 Haynes	B	.05	.10	<.005	.005	.08	18.15	51.52	.99	.57	3.13	5.14	.40	.02	-	bal	IVM: VAR	Mill Annealed

Table 2

Heat Treatments

Conventional	Annealed for 1 hr at 954 deg C, He cooled[a] to room temperature. Aged 8 hr at 728 deg C, furnace cooled 56 deg C/hr to 649 deg C, aged at 649 deg C for 10 hr, He cooled to room temperature.
Modified	Solution annealed for 1 hr at 1093 deg C, furnace step cooled at 38 deg C/hr to below 538 deg C, He cooled to room temperature. Aged 4 [illegible] at 718 deg C, step cooled at 38 deg C/h[illegible] deg C, aged 16 hr at 621 d[illegible] cooled to room temperature.

[a]He cooled in "cold wall" vacuum furnace.

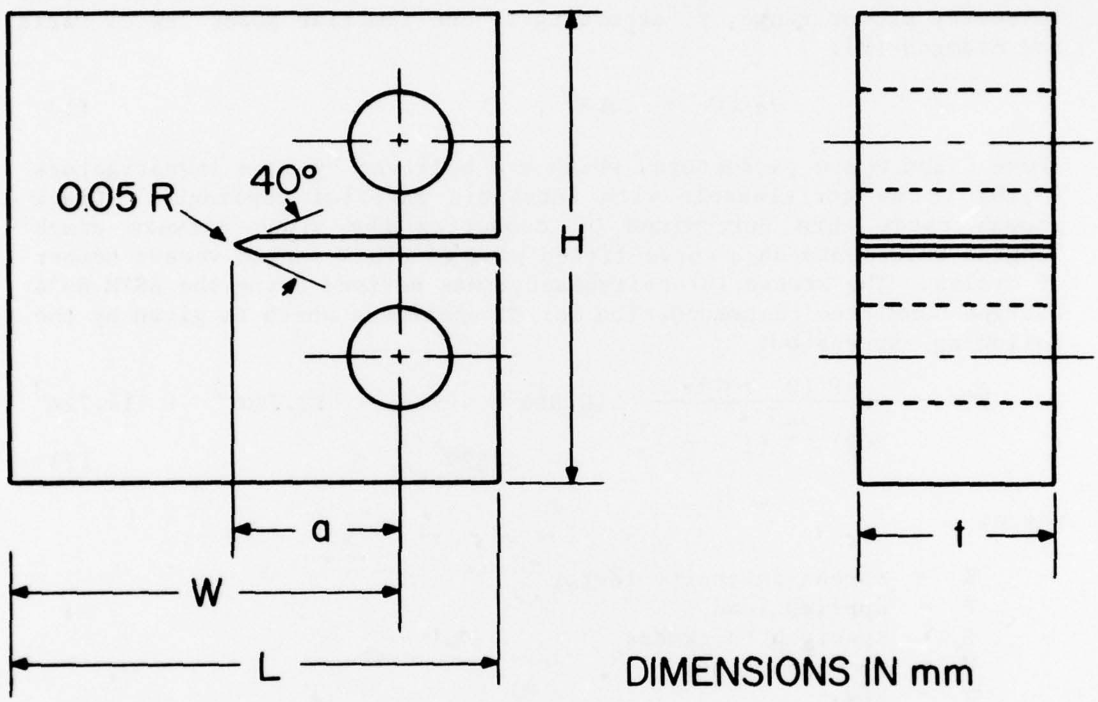

SIZE	L	H	t	a	W
0.5T	31.75	30.48	12.70	11.13	25.40
MOD.	40.64	30.48	10.16	13.72	34.29
IT	63.50	60.96	25.40	19.48	50.80

Fig. 1 - Dimensions of compact tension fatigue crack propagation specimens.

a temperature gradient along the fracture plane of less than 10 deg C.

The data obtained from the fatigue crack propagation tests were analyzed to yield crack growth rate, da/dN, as a function of the stress intensity factor range, K, according to the familiar power law of Paris and Erdogan (8):

$$da/dN = C \Delta K^m , \quad (1)$$

where C and m are parameters, which are believed by some investigators (9,10) to be correlatable with intrinsic material constants. Crack growth rates were determined by computing the slope between crack lengths increments on a curve-fitted plot of crack length versus number of cycles. The stress intensity factor was derived using the ASTM E-24 Fatigue Committee recommendation for CT specimens which is given by the following expression:

$$K = \frac{P\,(2 + \alpha)}{B(W)^{1/2}\,(1 - \alpha)^3}\,(0.886 + 4.54\alpha - 13.32\alpha^2 + 14.72\alpha^3 - 5.62\alpha^4), \quad (2)$$

where:

K = stress intensity factor
P = applied load
B = specimen thickness
W = specimen width
α = a/W.

Microstructural Analysis and Fractography

Various techniques were employed to examine the microstructures and identify the intermetallic phases present. The microstructures produced by the heat treatments were characterized by optical and scanning electron microscopy (SEM) of polished and etched metallographic sections, and by transmission electron microscopy (TEM) of thin foils. In a separate study, Evers, et al. (11) conducted energy dispersive x-ray analysis, x-ray fluorescence, and x-ray diffraction analysis of electrolytically extracted phases from Heat B material. Specimen fracture surfaces were examined using SEM procedures to determine the mode of failure. The surfaces were then electrolytically etched and reexamined to evaluate the correspondence between the various precipitated phases and the fracture mode.

Deformation Mechanisms

The relationship between the microstructure and deformation behavior was investigated by SEM analysis of fatigue fracture surfaces. The characteristics of the plane-strain deformation processes active at 427 and 593 deg C were examined in air and vacuum using a technique similar to that of Hahn and Rosenfield (11). In the present work,

test strips 17.7 mm wide by 1.3 mm thick were electropolished prior to being deformed in three-point bending to a nominal maximum fiber strain of 30 percent. It has been reported (12) that patterns of deformation similar to the flow at the root of a crack can be simulated with plastic bending. With this technique, the large plastic strain gradient in the thickness direction confines flow to the X-Y plane to produce quasi-plane strain conditions. It is considered that this technique simulates conditions near the free surface of the crack, if not the triaxial stress in the plastic enclave some distance ahead of the crack tip.

RESULTS

Microhardness

Room temperature microhardness measurements were made on coupons in the as-received condition and after the conventional and modified heat treatments. These examinations were conducted to assess the hardness and relative strength of the microstructures produced by the two heat treatments. Average values of the mesurements are shown in Table 3 for Heat A and B material. Considerable scatter was evident between individual hardness measurements. However, the averages in Table 3 of multiple measurements are consistent and indicate that the conventional heat treatment produced higher hardness values in both heats.

Fatigue Crack Propagation

The fatigue program was undertaken to examine the effect of heat treatment, test temperature, and hold time on the fatigue crack propagation (FCP) response of two heats of Alloy 718. The data obtained from the fatigue crack propagation tests are shown in Figs. 2 through 6.

Results of fatigue crack propagation investigation of the Alloy 718 material, designated as Heat A, are shown in Fig. 2. The effect of the conventional and modified heat treatments on the fatigue crack propagation resistance of this heat were evaluated at 427 and 593 deg C. The most significant effect of heat treatment was seen at 427 deg C where a large increase in crack propagation resistance was realized from the modified heat treatment. At 593 deg C, the fatigue properties of this heat of Alloy 718 appear to be similar or slightly reduced by the modified heat treatment. Similar FCP evaluations of the effect of heat treatment, which were made for the Alloy 718 material designated Heat B, are shown in Fig. 3. In this instance, the modified heat treatment produced an increase in the crack propagation resistance of the Heat B material at both 427 and 593 deg C.

Comparisons of the fatigue properties of the two heats of Alloy 718 are shown in Figs. 4 and 5 for the conventional and modified heat treatment conditions, respectively. The results in Figs. 4 and 5 show that, for comparisons made on the basis of temperature, Heat A material exhibits superior fatigue crack propagation resistance in comparison to that of

Table 3

Average Diamond Pyramid Hardness Values (Vickers) for Alloy 718, Heats A and B

Heat	Condition	DPH Numbers Small Grains $15 \mu m$	Large Grains $125 \mu m$
A	As-Received	331	325
	Conventional H.T.	486	468
	Modified H.T.	-	468
B	As-Received	281	240
	Conventional H.T.	470	454
	Modified H.T.	-	422

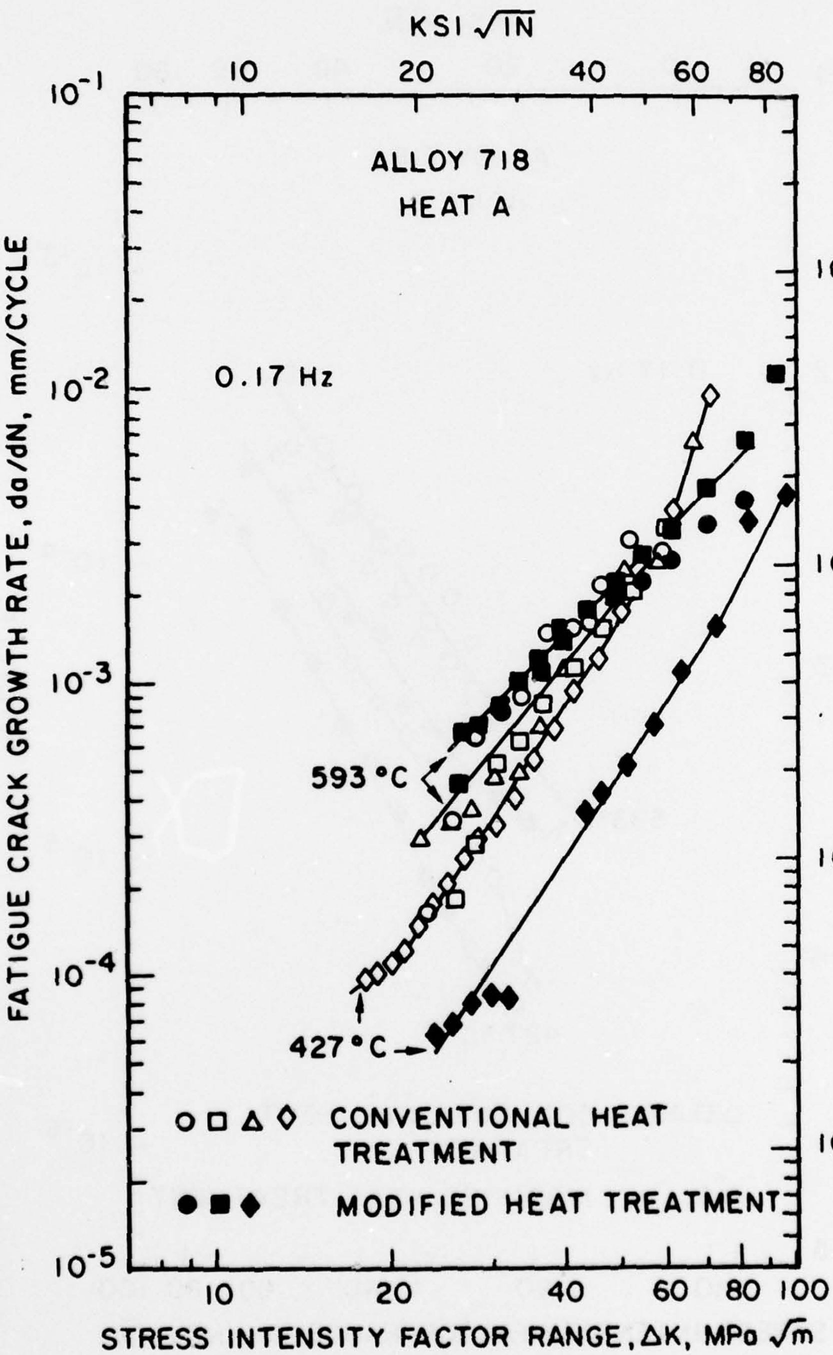

Fig. 2 - Effect of heat treatment on fatigue crack propagation rate in air for Heat A Alloy 718 at 427 and 593 deg C.

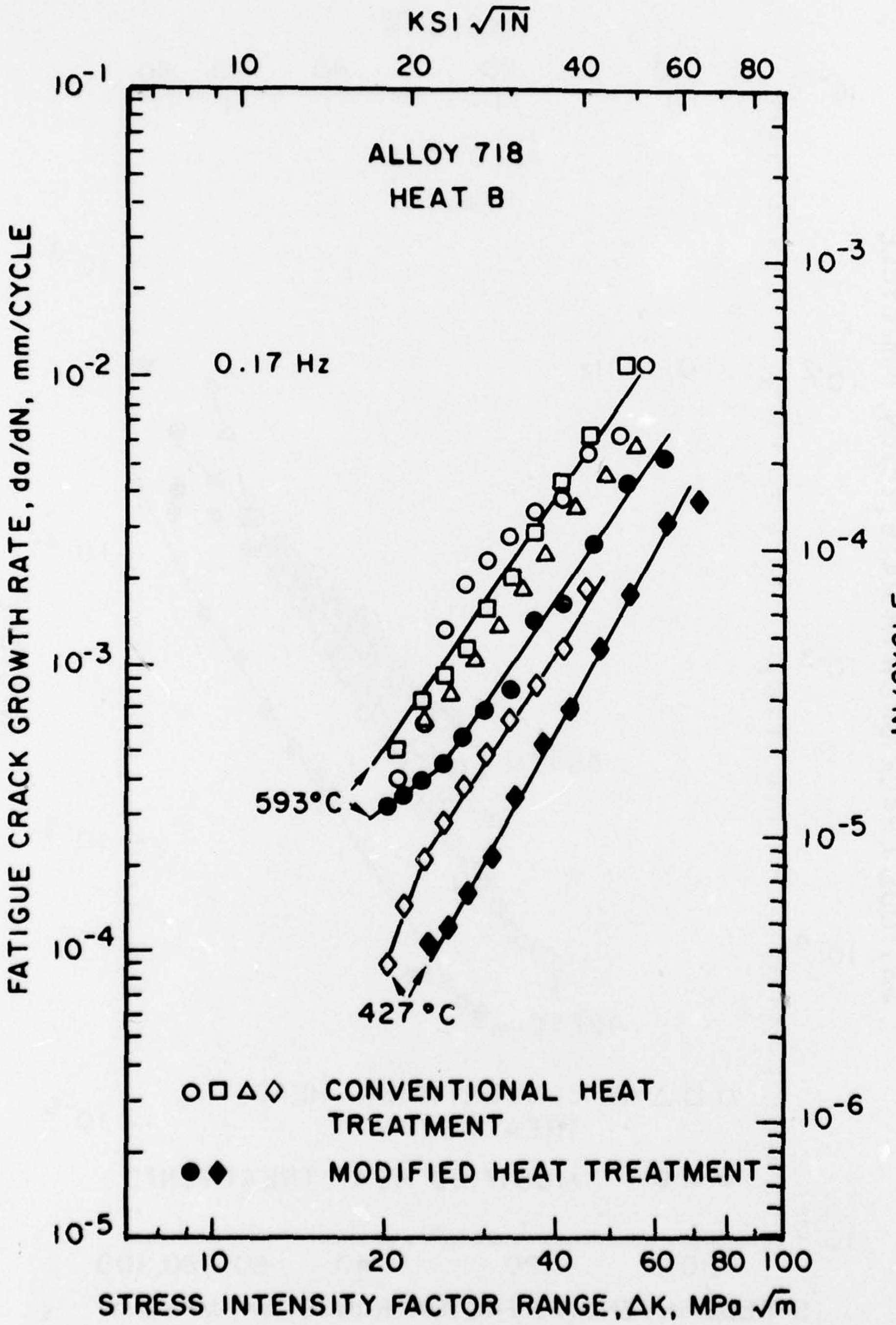

Fig. 3 - Effect of heat treatment on fatigue crack propagation rate in air for Heat B Alloy 718 at 427 and 593 deg C.

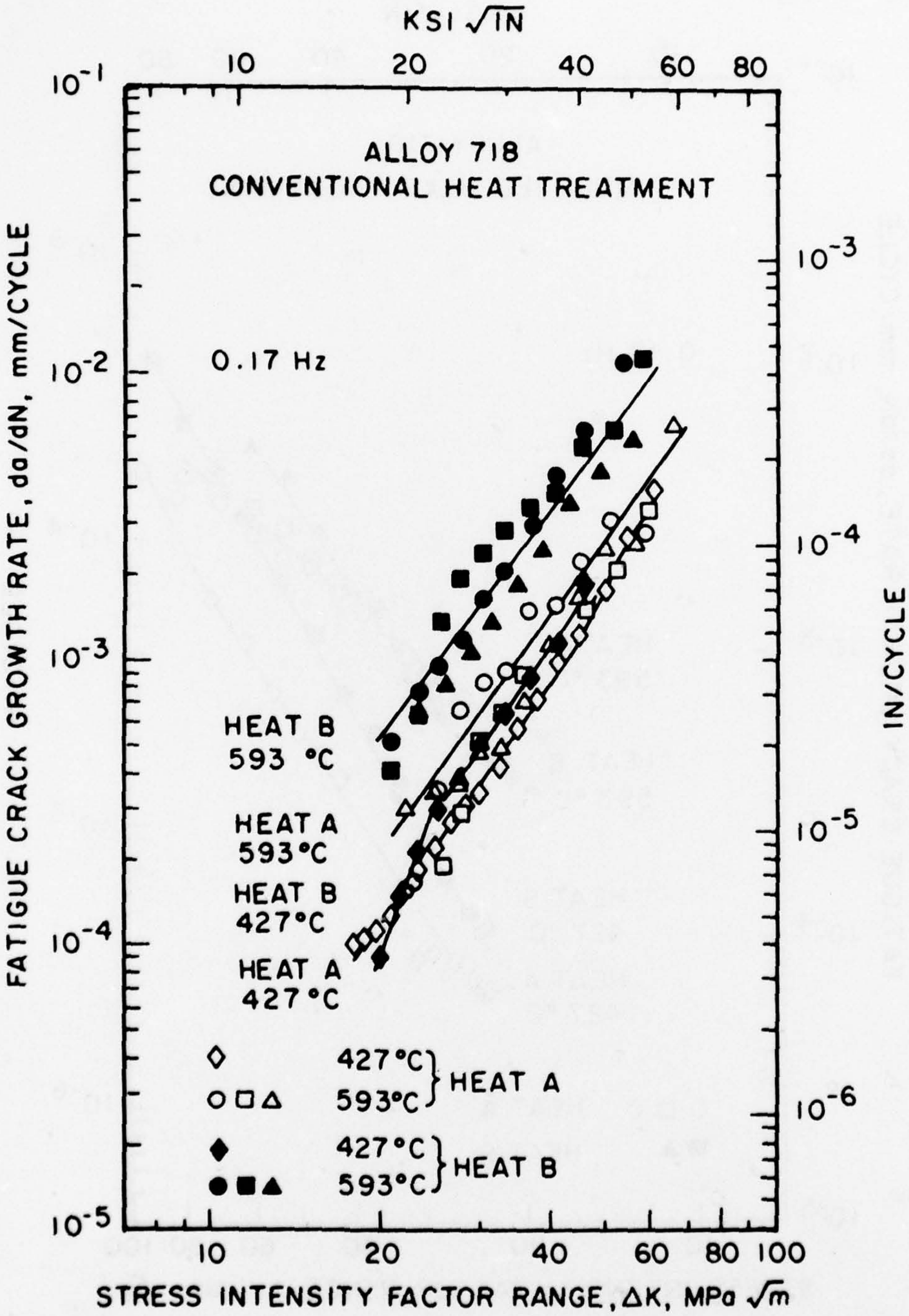

Fig. 4 - Comparison of fatigue crack propagation rates at 427 and 593 deg C in air for Heat A and Heat B Alloy 718 given the conventional heat treatment.

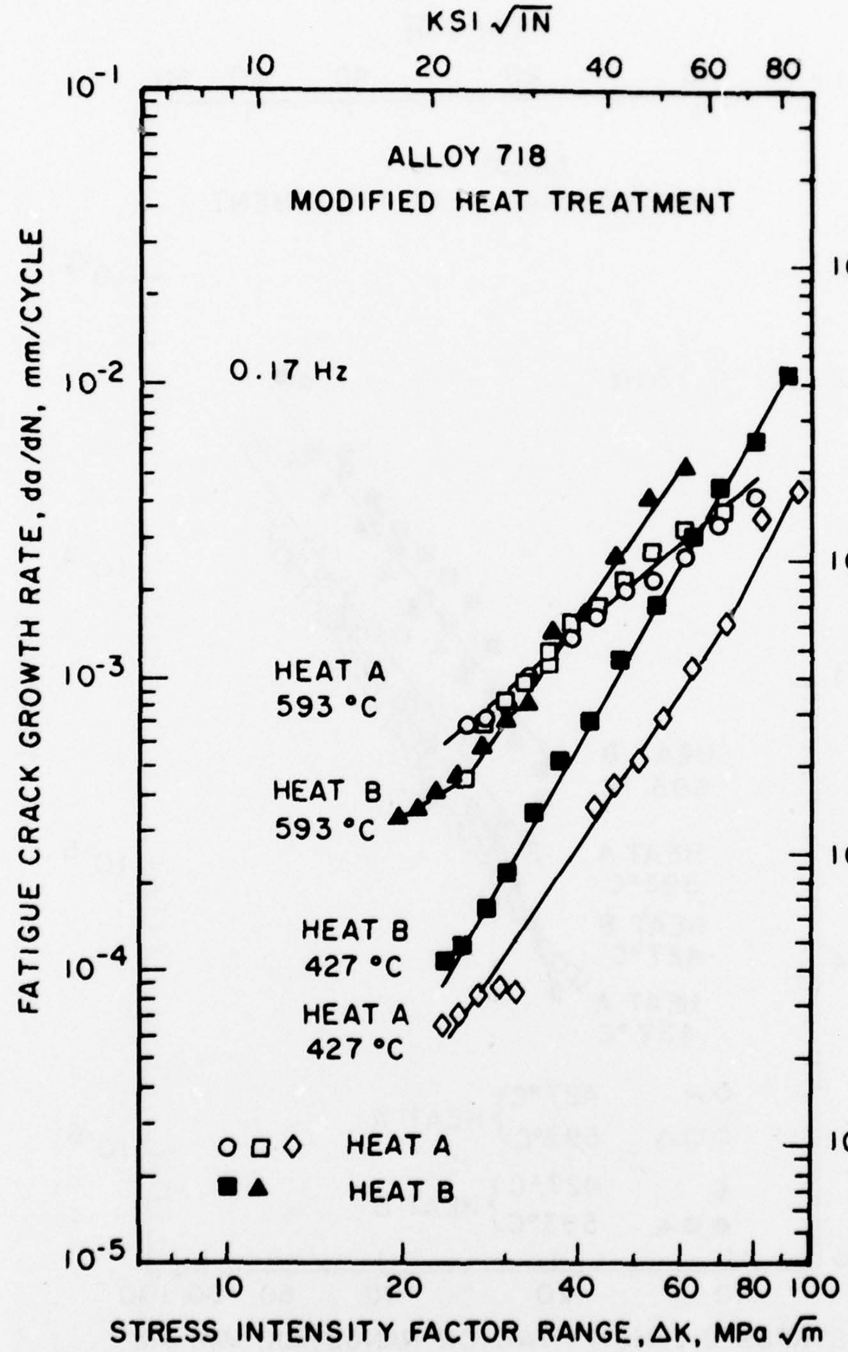

Fig. 5 - Comparison of fatigue crack propagation rates at 427 and 593 deg C in air for Heat A and Heat B Alloy 718 given the modified heat treatment.

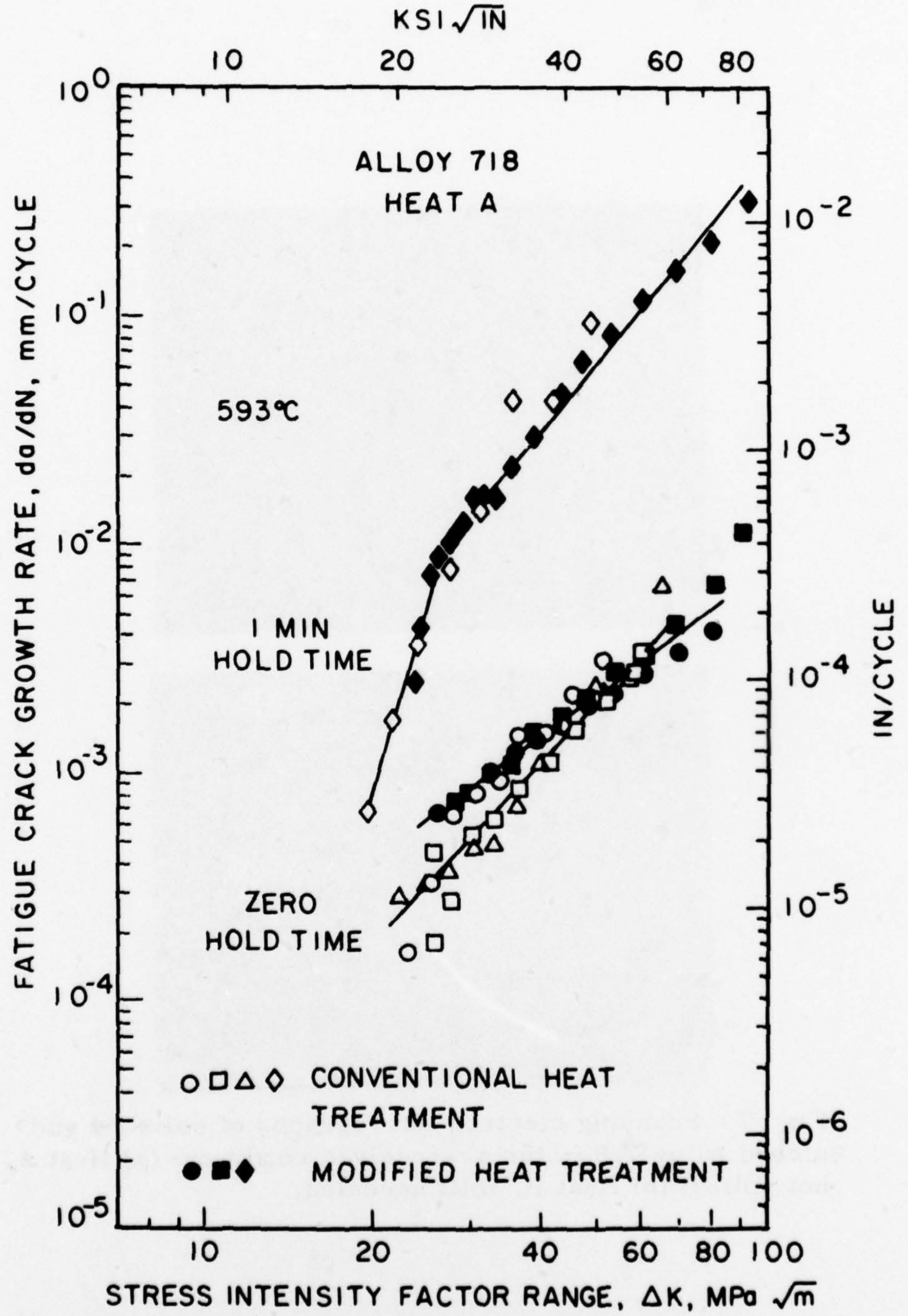

Fig. 6 - Effect of one minute hold time on fatigue crack propagation rates at 593 deg C in air for Heat A Alloy 718 given the conventional and modified heat treatments.

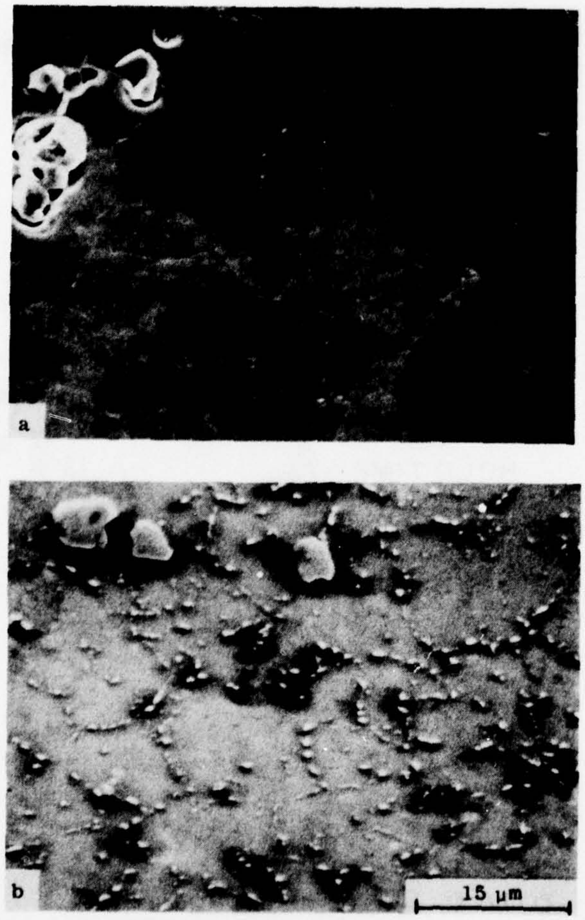

Fig. 7 - Scanning electron micrographs of polished and etched Alloy 718 in the as-received condition: (a) Heat A, hot rolled; (b) Heat B, mill annealed.

Heat B. Thus, the seemingly beneficial effect of the modified heat treatment on the Heat B material at 593 deg C may not be particularly significant from an engineering standpoint due to the intrinsically inferior fatigue properties of this heat of Alloy 718.

Other investigations (6,13) have studied the effect of cyclic frequency on the fatigue properties of conventionally heat treated Alloy 718. These studies have shown that the fatigue properties are cycle dependent at rates less than approximately 0.067 Hz (4 cpm). In the present work, the effect of hold time on FCP response and failure mechanism was investigated for the frequency interval of 0.17 to 0.015 Hz (10 to 1 cpm) by conducting hold time tests at 593 deg C for Heat A material in both the conventional and modified heat treatment conditions. In Fig. 6, the effect of a 1.0 minute hold (0.015 Hz), imposed at the peak tensile load during each cycle, on the fatigue propagation rate in the Heat A alloy is shown for the conventional and modified conditions. Although there is considerable effect of a one minute tensile hold period, the magnitude of the effect is similar for both heat treatments.

Microstructural and Fractographic Observations

The microstructure and the fracture surfaces of the tested specimens of Alloy 718 were examined to provide further insight into the complex relationships that exist between microstructures, deformation processes and crack propagation behavior of this alloy at elevated temperatures. Light and electron microscopy techniques were employed to determine the effect of heat treatment on microstructure and fracture appearance. The results of these examinations are shown in Figs. 7 through 11 for the conventional and modified heat treatment conditions.

As-Received Condition

The photomicrographs in Figs. 7a and 7b represent the general as-received microstructures for the Heat A and Heat B materials. The major feature of both Heat A and Heat B microstructures,were the large carbides, the fine grain boundary precipitates, and the similar grain size for both heats of material. The most salient feature apparent from the microstructures, which would indicate a significant difference between the properties of the two heats, was the prevalence of the grain boundary phase in the Heat B alloy in the as-received condition, Fig. 7b.

Conventional Heat Treatment

The effect of heat treatment on the microstructure and fracture appearance of the two heats of Alloy 718 is presented for the conventional heat treatment in Figs. 8 and 9. For the Heat A material, the conventional (954 deg C anneal plus 718/649 deg C age) heat treatment produced a duplex microstructure with grain sizes of approximately 15 and 125 μm as shown in Fig. 8a. SEM representation of the fracture surfaces of fatigue specimens tested at 427 deg C, Fig. 8b, and 593 deg C, Fig. 8c, show contouring which appears to be

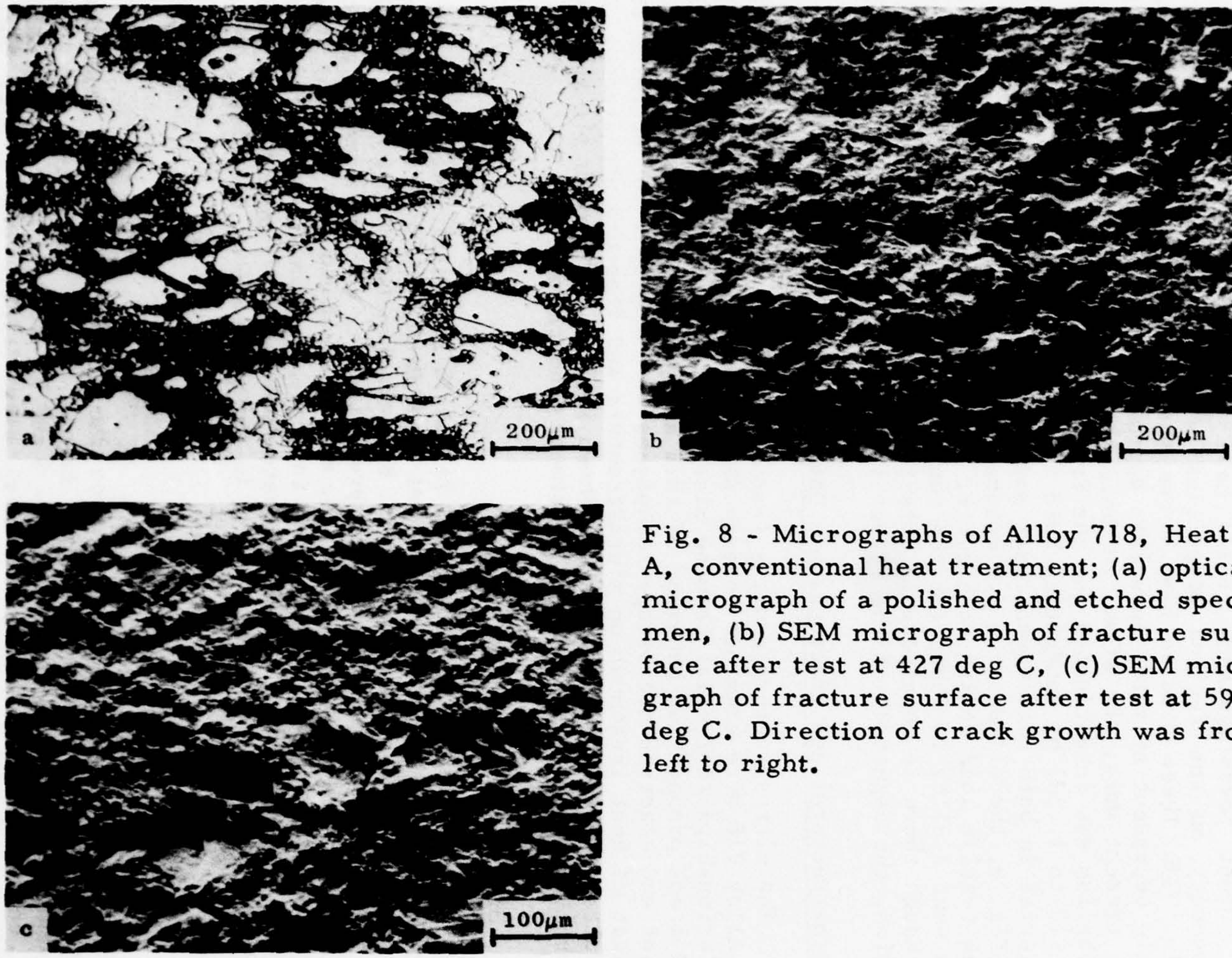

Fig. 8 - Micrographs of Alloy 718, Heat A, conventional heat treatment; (a) optical micrograph of a polished and etched specimen, (b) SEM micrograph of fracture surface after test at 427 deg C, (c) SEM micrograph of fracture surface after test at 593 deg C. Direction of crack growth was from left to right.

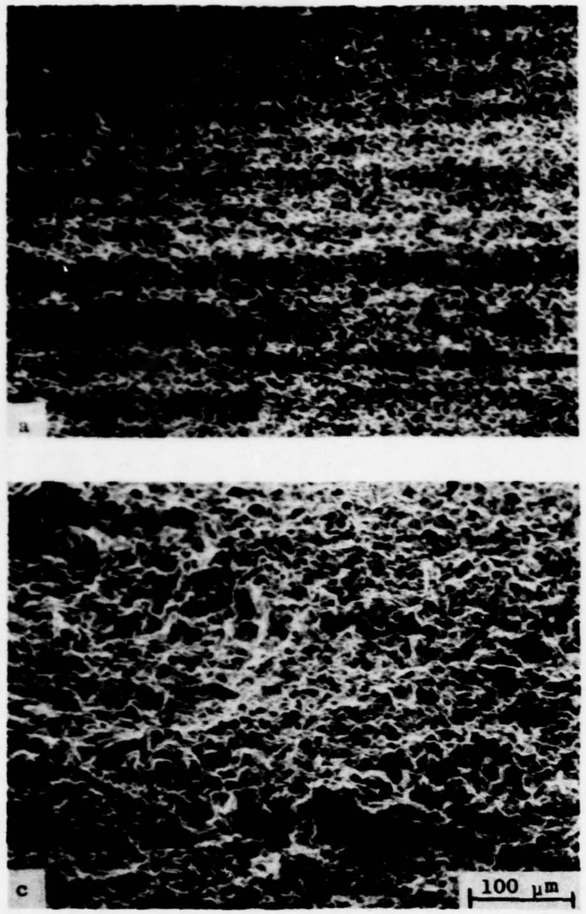

Fig. 9 - SEM micrographs of Alloy 718, Heat B, conventional heat treatment; (a) polished and etched sample, (b) fracture surface after test at 427 deg C, (c) fracture surface after test at 593 deg C. Direction of crack growth was from left to right.

morphologically similar to the microstructure. Fracture surfaces were flat and devoid of shear lips and, together with the observation that the surfaces bore a close resemblance to the microstructure, suggest that the crack propagated without appreciable plastic deformation. There appeared to be no preponderance of small or large grains on the fracture surface to indicate preferential cracking characteristics. At 427 and 593 deg C, fracture of the large grains was clearly transgranular with striations and river patterns indicating possible crystallographic cleavage. At 593 deg C, the small grains adjacent to the large grains exhibited an intergranular fracture appearance. However, when the crack propagated through an area composed of small grains the fracture appeared to be transgranular for the Heat A material.

Micrographs for the Heat B material given the conventional heat treatment and tested at 427 and 593 deg C are shown in Fig. 9. The microstructure was considerably more homogeneous, Fig. 9a, than in Heat A with a grain diameter approximately equal to the as-received grain size of 15 μ m. The characteristic banding common to Alloy 718 was clearly evident. The grain boundary phase was slightly coarsened by the conventional heat treatment, but it appeared that the grain boundary phase present in the Heat B alloy before heat treatment had stabilized the grain size and had resulted in a more uniform structure than in the Heat A material. The fracture surfaces of the Heat B material at 427 and 593 deg C, Figs. 9b and 9c, also appeared to be microstructurally dependent, and the fracture mode was predominantly transgranular. No outstanding microstructural evidence was found which could explain the reduced crack propagation resistance of the Heat B material, as demonstrated in Fig. 4. After the conventional heat treatment, both heats were heavily decorated by grain boundary phases and large carbides were found throughout the matrix. The grain size did not appear to be significantly different and the transgranular crack propagation mode was common to both heats.

Modified Heat Treatment

In the modified heat treatment, one of the principal functions of the solution anneal is the ductilization of the alloy by depletion of the Laves phase during heating above 1040 deg C. The Heat A microstructure resulting from the modified (1093 deg C anneal, 718/621 deg C age) heat treatment is shown in Fig. 10. The microstructure appeared fully recystallized with many annealing twins. The modified treatment produced a fairly uniform grain size of approximately 125 μ m, Fig. 10a. with many large carbides in evidence throughout the microstructure. At 427 deg C, the fracture surface showed considerable faceting indicating a crystallographic cleavage mode of fracture, Fig. 10b. In contrast at 593 deg C, Fig. 10c, the fracture mode was clearly intergranular with appreciable secondary cracking along grain boundaries. An intergranular fracture mode also was observed for the one minute hold time test at 593 deg C. Whereas the conventional heat treatment showed little dependence of fracture mode on test

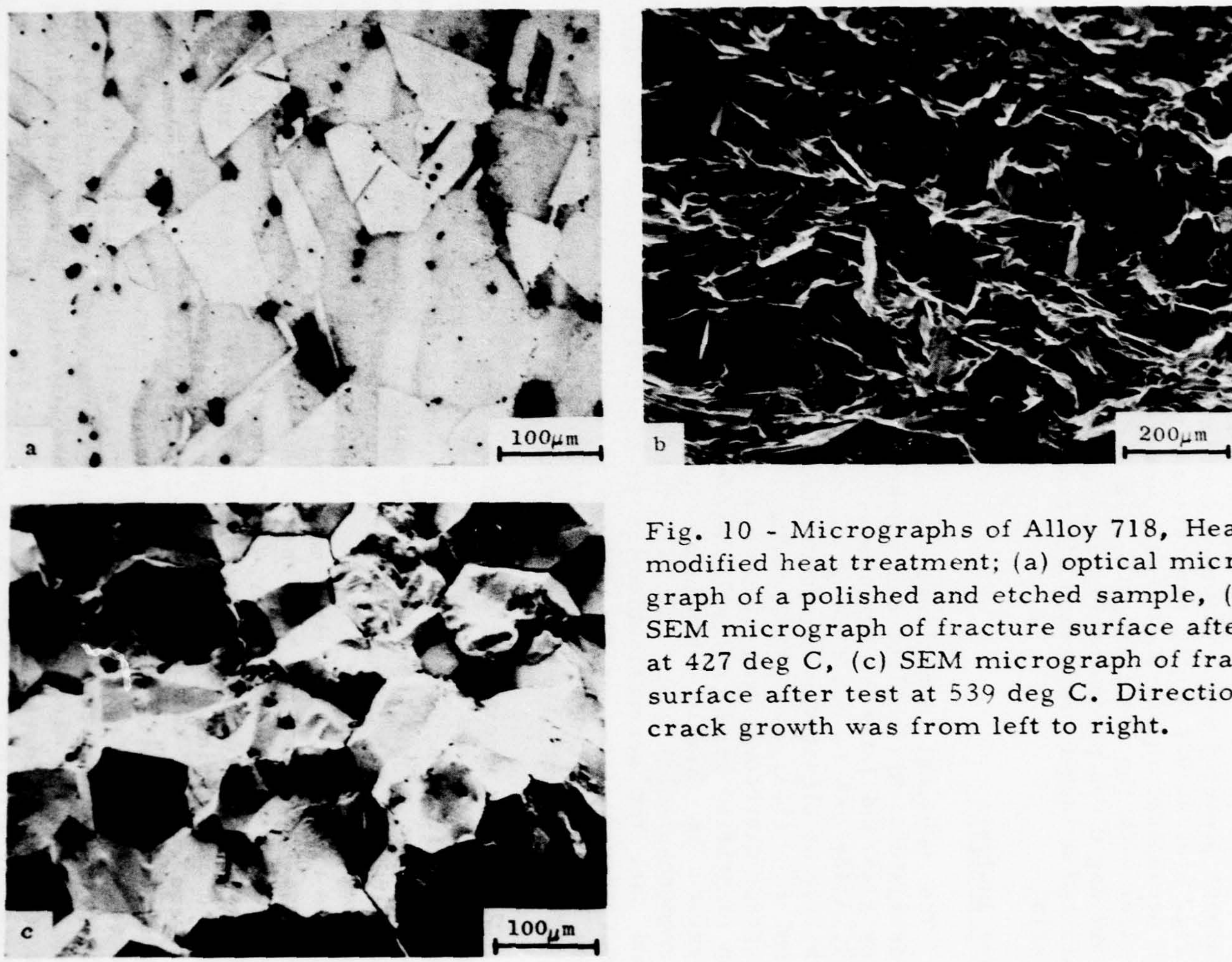

Fig. 10 - Micrographs of Alloy 718, Heat A, modified heat treatment; (a) optical micrograph of a polished and etched sample, (b) SEM micrograph of fracture surface after test at 427 deg C, (c) SEM micrograph of fracture surface after test at 539 deg C. Direction of crack growth was from left to right.

temperature, the modified treatment produced a microstructural condition which was highly sensitive to test temperature.

A similar effect was seen for the Heat B material given the modified heat treatment. The higher temperature anneal of the modified treatment produced grain growth and cleaner grain boundaries as shown in Fig. 11a. At 427 deg C, fracture was predominantly transgranular but with occasional intergranular fracture areas where grain boundaries were parallel with the fracture path, Fig. 11b. The mixed mode of failure at 593 deg C was predominantly intergranular, Fig. 11c, but clearly exhibited a larger proportion of transgranular failure mode than Heat A material.

Phase Analysis

The physical metallurgy of Alloy 718 has been extensively investigated. While first considered to be a gamma prime strengthened alloy (14) and later to be primarily gamma double prime strengthened (15), Alloy 718 is now thought to derive its high strength and phase stability at elevated temperatures from a morphological mixture of both γ' and γ'' (16). In addition to these strengthening phases, other important microconstituents, such as Laves phase, CbC, and Ni_3Cb, have been identified in the Alloy 718 microstructure. Because precipitation behavior is highly dependent on alloy composition (14,16), thermomechanical history (17,18), and heat treatment (15,19), it was found that the generalization of precipitation reactions from time-temperature diagrams or metallographic studies established for other Alloy 718 compositions was not reliable. Therefore, a phase study for one of the present alloys was undertaken.

The major precipitate phases in the Heat B alloy were investigated by Evers, et al. and the results of that study are presented in detail elsewhere (11). Briefly, electrolytic extraction methods were used to separate two major phases from the matrix. These two phases were identified by x-ray diffraction techniques to be CbC and a hexagonal A_2B type compound, probably a Laves phase. Analysis of the extraction residues revealed that the modified heat treatment reduced the fractional amount of the hexagonal phase in the residue as compared to the as-received alloy. X-ray fluorescence analyses confirmed these findings. Energy dispersive x-ray analyses of the residues indicated that the composition of the carbide phase was (Cb,Ti)C. This phase is the large rounded or blocky precipitate in Fig. 12. The Laves phase composition was $(Ni,Fe,Cr)_2(Cb,Ti)$ which is consistent with the x-ray fluorescence results. This phase is the small precipitates in Fig. 12. It is probable that the grain boundaries contain CbC in addition to the Laves phase. The microstructures of the materials given the modified heat treatment contained grain boundary films, presumably CbC, as reported by Eiselstein (14). Ni_3Cb needles were seen in varying amounts in all heat treated conditions, but to the largest degree in the conventionally heat treated, Heat A material. For this condition, Ni_3Cb needles were observed in the microstructure, and the shear lips of fracture surfaces were heavily decorated with these needles.

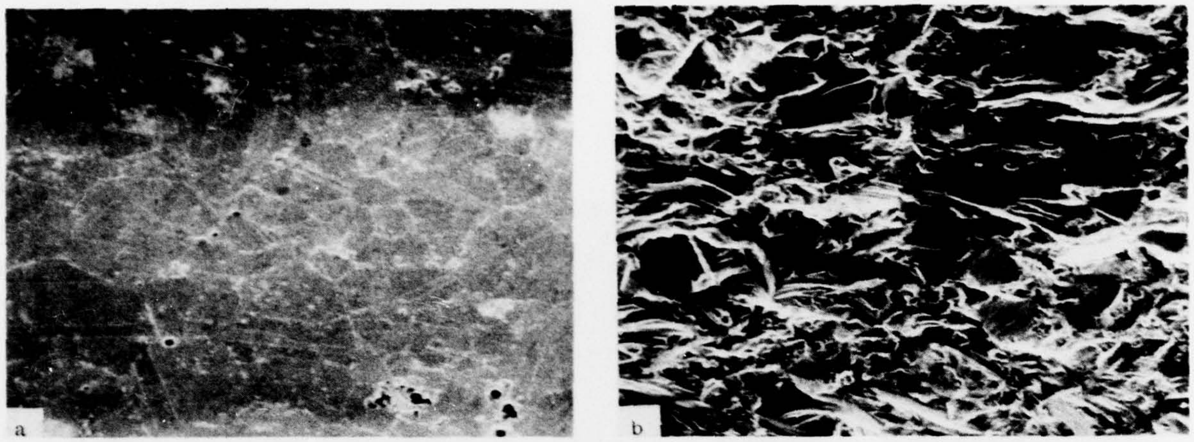

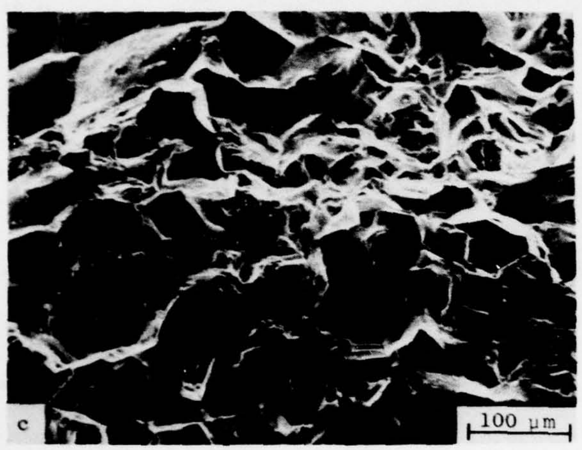

Fig. 11 - SEM micrographs of Alloy 718, Heat B, modified heat treatment; (a) polished and etched sample, (b) fracture surface after test at 427 deg C, (c) fracture surface after test at 593 deg C. Direction of crack growth was from left to right.

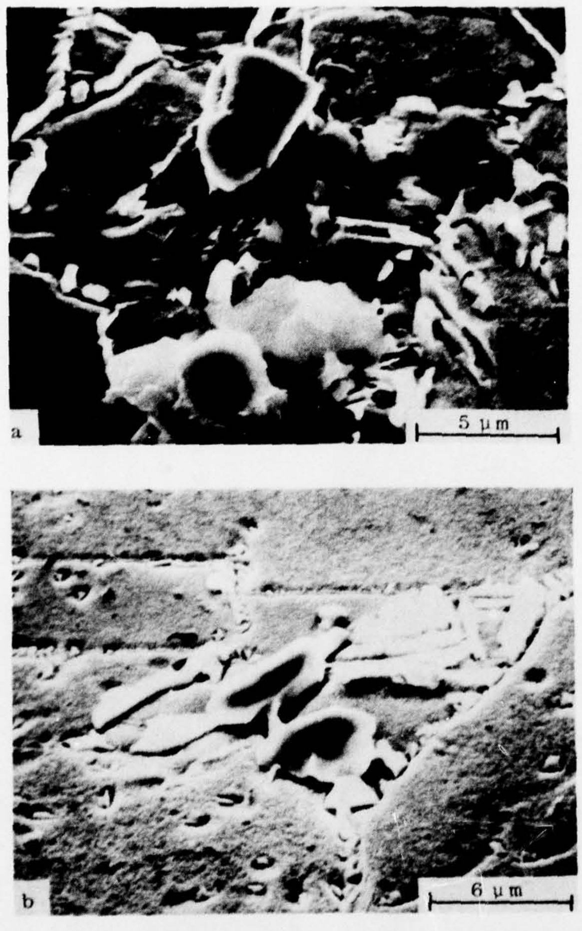

Fig. 12 - SEM micrographs of Alloy 718, Heat A microstructure showing the nature of (a) the large Cb carbides and grain boundary phases (Laves and CbC) in the conventional heat treatment condition, and (b) the large Cb carbides, fine grain boundary phases, and carbide films (CbC) in the modified heat treatment condition.

TEM Results

TEM photomicrographs which revealed the size and distribution of γ'' precipitates in the Alloy 718 matrix are shown in Fig. 13. Particle size analyses from dark field micrographs of Heat A material in the conventional heat treatment condition indicated a mean precipitate diameter of approximately 14.1 nm and a density of 1.4×10^{16} cm^{-3}. Size measurements for material given the modified heat treatment indicated a mean precipitate diameter of approximately 29.8 nm and a density of 6.5×10^{14} cm^{-3}. Similar results were obtained for Heat B material. The TEM results are tabulated in Table 4.

Deformation Mechanisms

The details of the plane strain deformation processes active at 427 and 593 deg C were examined in air and vacuum by plastically deforming thin strips of the Heat A alloy in three-point loading. SEM photomicrographs of plane strain specimen surfaces plastically deformed in vacuum at 427 and 593 deg C are shown in Fig. 14. It can be seen in Figs. 14a and 14b that the conventional heat treatment produced a tendency for localized, planar slip, whereas in the modified condition, Fig. 14c and 14d, a more uniform homogeneous deformation is apparent. Thus, in vacuum, the modified heat treatment reduced the tendency for localized planar slip which should result in enhanced crack propagation resistance. It is quite well known, however, that surface deformation and slip in fatigue are affected by environment. Since the fatigue tests in this study were conducted in air, a similar series of plane strain bend evaluations were conducted in air at 427 and 593 deg C to determine the effect of environment on the deformation processes.

For deformation in air at 427 and 593 deg C, Figs. 15a and 15b, show typical deformation processes prevalent on plane strain specimen surfaces of material given the conventional heat treatment. In air at 427 deg C, Fig. 15a, the nature of the slip deformation was similar to that in vacuum at 427 deg C where localized planar slip was the prevalent mechanism. However, the air environment appeared to have produced a more even distribution of slip through the duplex grain size, whereas in vacuum, the slip lines were generally found within the larger grains. Under these conditions, the fracture mode was predominantly transgranular as would be suggested by the tendency for slip localization and large slip offsets shown in Fig. 15a. At 593 deg C, Fig. 15b, it was still evident that slip tended to concentrate on localized planes, but there also was a considerable amount of grain boundary cracking in small grains adjacent to large grains. The intergranular cracking was seen to be associated with the intersection of persistent slip lines with grain boundaries or fractured precipitates within the grain boundaries. The mixed fracture mode in Fig. 8c concurs with the observed planar slip and grain boundary cracking seen in Fig. 15b.

The effect of environment on slip deformation was more pronounced in the material given the modified heat treatment, Figs. 15c and 15d.

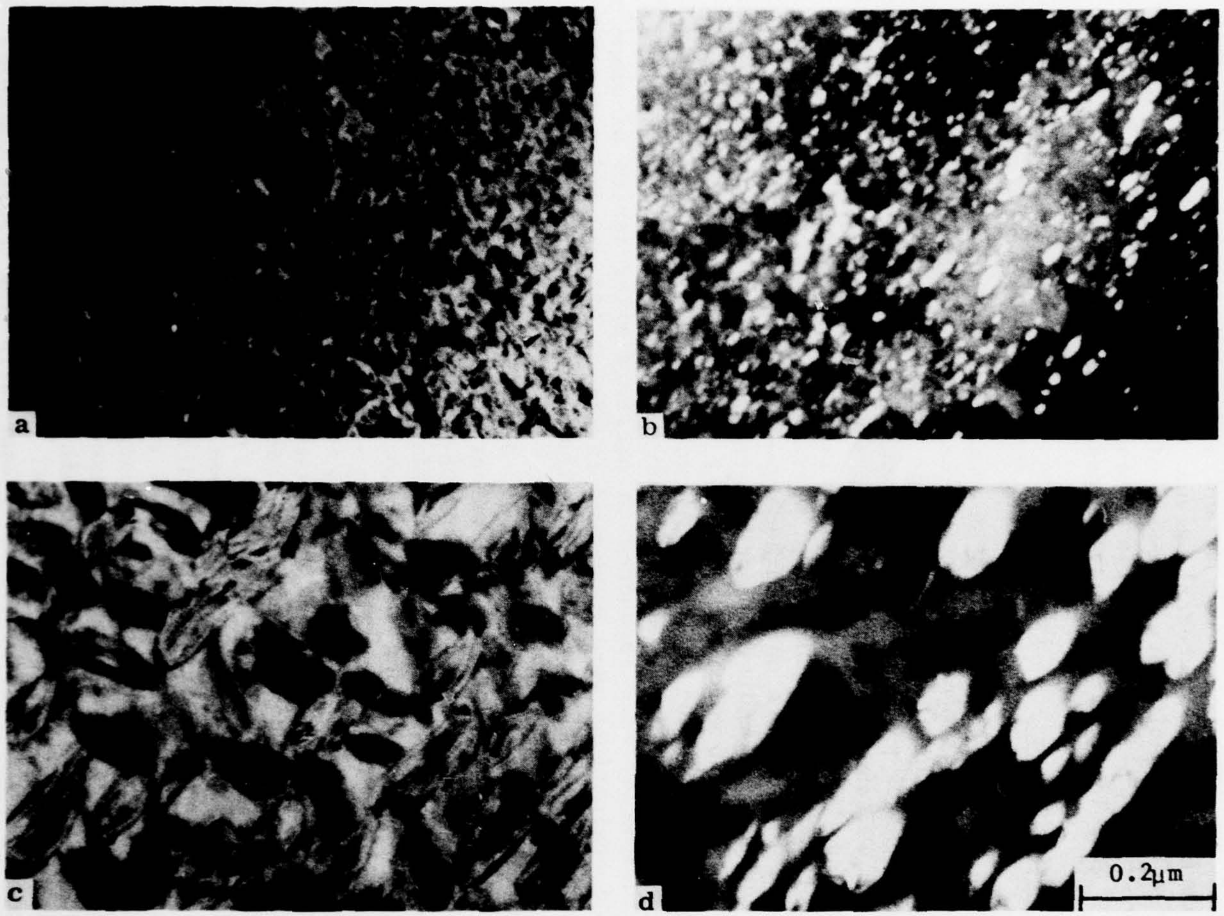

Fig. 13 - TEM micrographs of Alloy 718, Heat A showing γ'' precipitate microstructure: conventional heat treatment condition, (a) bright field image, (b) dark field image; modified heat treatment condition, (c) bright field image, and (d) dark field image.

Table 4

Mean Diameter and Density of γ'' Precipitates in Alloy 718

Heat	Heat Treatment	Mean Diameter (nm)	Density (#/cm^3)	Volume Fraction[a] (%)
A	Conventional	14.1	1.4×10^{16}	1.03
	Modified	29.8	6.5×10^{14}	0.45
B	Conventional	7.9	1.7×10^{16}	0.22
	Modified	23.7	5.5×10^{14}	0.19

[a]Assumes constant aspect ratio of dia/thickness = 3.

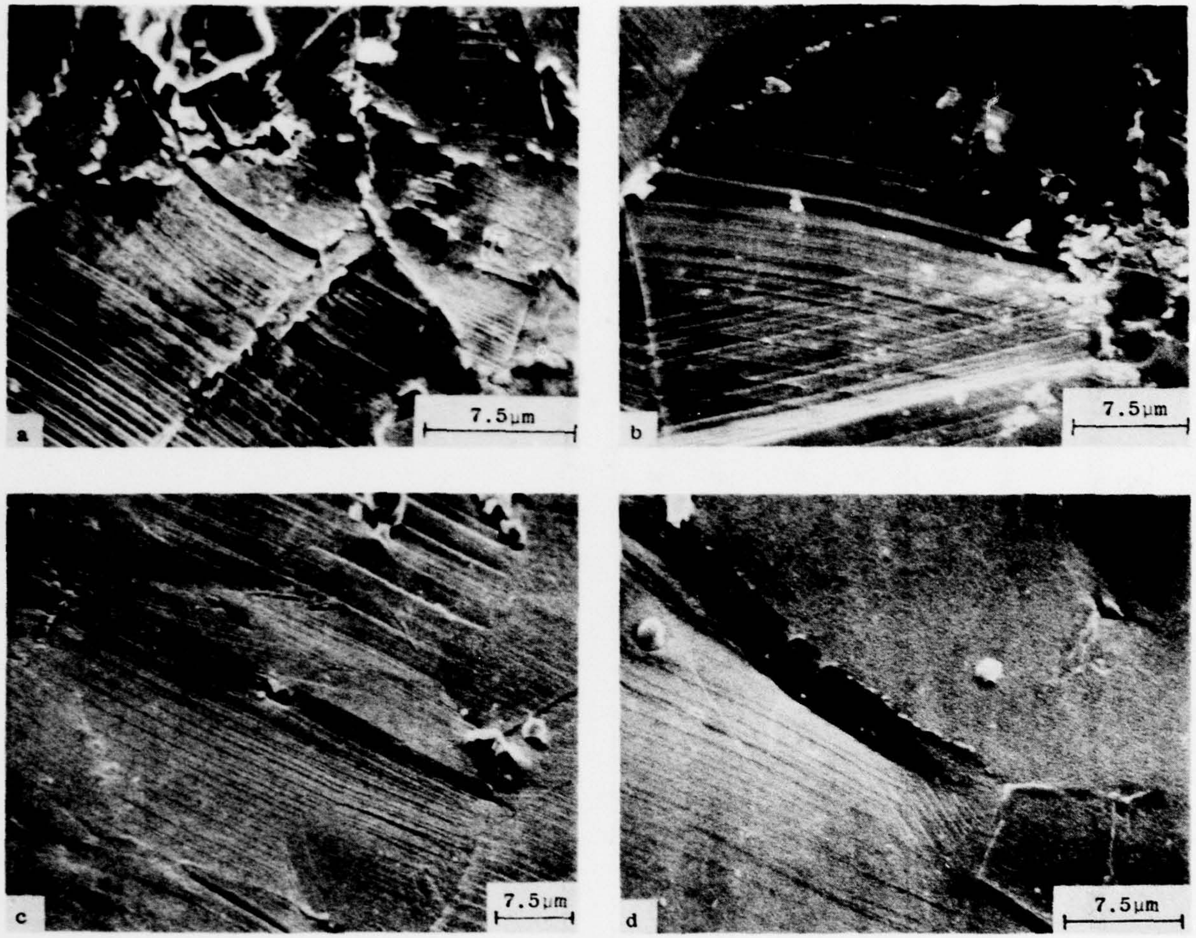

Fig. 14 - SEM micrographs of slip behavior in plane strain bend samples of Alloy 718, Heat A, deformed in vacuum: (a) conventional heat treatment, 427 deg C; (b) conventional heat treatment, 593 deg C; (c) modified heat treatment, 427 deg C; (d) modified heat treatment, 593 deg C.

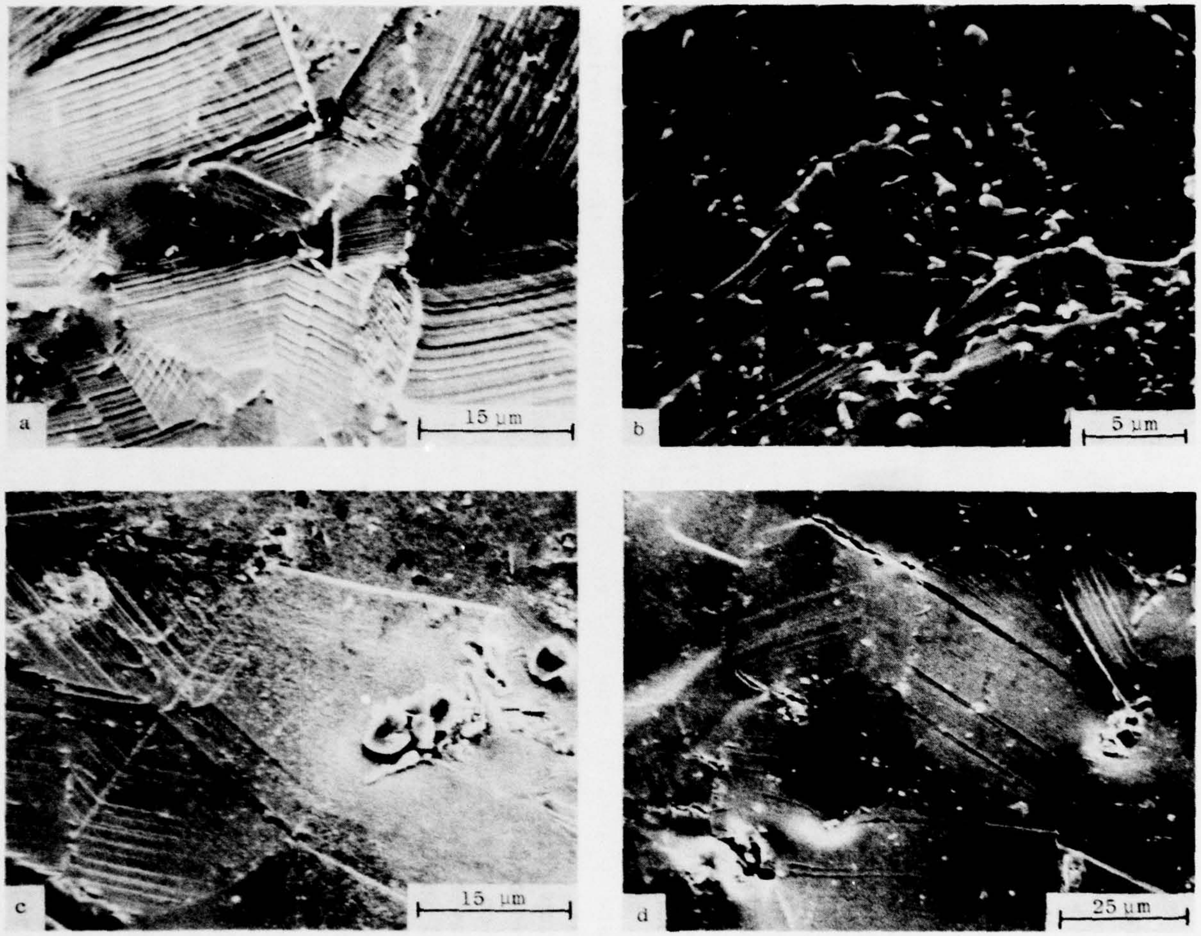

Fig. 15 - SEM micrographs of slip behavior in plane strain bend samples of Alloy 718, Heat A, deformed in air: (a) conventional heat treatment, 427 deg C; (b) conventional heat treatment, 593 deg C; (c) modified heat treatment, 427 deg C; (d) modified heat treatment, 593 deg C.

Deformation in air, in contrast to vacuum, produced a more planar type slip with large slip offsets. At 427 deg C, Fig. 15c, slip appeared to produce offsets at twin boundaries and would be expected to produce fracture surfaces similar to that shown in Fig. 10b. At 593 deg C, deformation occurred by grain boundary separation, Fig. 15d. Slip line deformation appeared to be related to the grain boundary cracks; however, it was not certain whether the grain boundaries cracked first or separated because of the interaction of the slip with the grain boundary. It would be expected, then, that the specimens given the modified heat treatment and tested in air would exhibit intergranular failure as shown in the SEM micrograph, Fig. 10c.

DISCUSSION

The results of this study show that the primary effect of the modified heat treatment was to significantly increase the resistance of Alloy 718 Heat A material to fatigue crack propagation at 427 deg C while decreasing the resistance at 593 deg C, Fig. 2 and Figs. 4 through 6. In a previous study, James (6) has reported similar effects of the modified heat treatment on fatigue crack propagation resistance of Alloy 718. The present results also show that the modified heat treatment had a profound influence on the deformation mode of Heat A material in plane strain bending. Since it is well known that the mechanical properties of nickel-base alloys are strongly dependent on microstructure, the proper explanation of the fatigue crack propagation response of Alloy 718 requires an understanding of the effect of precipitate phases on the deformation mechanisms. In the following paragraphs, the influence of microstructure on the fatigue crack propagation response of Alloy 718 is discussed on the basis of the plane strain deformation results for the Heat A material. Since the deformation results for the Heat B material are not yet available (20), the improved fatigue crack propagation resistance of this material at 593 deg C in the modified heat treatment condition cannot be discussed completely. However, the probable causes of the fatigue crack propagation response of the Heat B material will be inferred from the Heat A results.

In general, two models of fatigue crack propagation have been proposed in which the crack grows as a consequence of cyclic hardening at the crack tip (21) or by a plastic blunting process (22). These models are similar in that regardless of whether the macroscopic fracture process is the result of "fracture of a blunted crack" or "flow-off" (23), the process takes place on a pair of intersecting slip planes. Hahn and Rosenfield (12) have demonstrated the usefulness of the plane strain bend technique for simulating the deformation at the root of a crack in aluminum alloys and, more recently, Michels and Floreen (24) have studied the relationship between the microstructures and deformation in a nickel-base alloy. The study of slip processes is very instructive since this process directly influences ductile fatigue crack propagation. Thus, the understanding of the relationship between the microstructure and deformation behavior, as evidenced from the

observations of the interactions of slip and precipitate phases in bend samples should aid in the correlation of these factors with the fatigue crack propagation properties of materials.

The slip behavior observed with the Alloy 718 bend specimens suggests that the improvement in FCP performance produced by the modified heat treatment is likely to be a result of the alteration of dislocation interaction with γ'' particles and grain boundaries. Comparison of the slip line appearance for the conventional and modified heat treatments at 427 deg C in vacuum, Fig. 14a and 14c, revealed that the modified heat treatment produced a microstructural condition conducive to homogeneous deformation which has been found (25,26) to result in significant improvements in crack growth resistance. This observed alteration of the slip mode suggests that deformation mechanisms analogous to processes in low γ' fraction alloys were active. In these alloys, plastic deformation may involve either the shearing or the bypassing of the γ' particles, depending on the particle size and distribution (27). The shearing of the matrix and the γ' particles by paired dislocations (a/2 $<110>$) produces heterogeneous slip, a mechanism characteristic of face-centered cubic materials. After particles are sheared, the resistance in that plane is reduced to subsequent slip so that extensive dislocation activity persists on that slip plane giving rise to characteristically intense slip traces and coarse slip offsets. Fournier and Pineau (26) foud that the increase in the homogeneity of the plastic deformation produced during fatigue of Alloy 718 was related to the concurrent increase in fatigue life. Their electron microscopy observations revealed that γ'' precipitates were sheared by partial dislocations by a process similar to the γ' particle dislocation interactions. In the modified heat treatment, the slower cooling rate produced γ'' particle coarsening, Fig. 13. These larger particles and the reduced volume fraction of precipitates would be expected to favor the bypassing of γ'' by dislocations. Under this mode of deformation slip will be relatively homogeneous and there will be less tendency for dislocation pile-ups and crack formation. In addition to the effect of the matrix on crack propagation, the grain boundaries may also produce a secondary contribution to the observed fatigue behavior.

Studies involving single and polycrystals have shown that grain boundaries may have an effect on the development of multiple slip and increased flow stress in polycrystals. The magnitude of these effects are related to the ability of the boundary to suppress clustered slip. It has been suggested (28) that increased flow stress is a result of multiple slip near grain boundaries which is caused by the back stress of piled-up dislocations in neighboring grains. An example of the nature of the interaction of slip and grain boundaries in the conventional heat treatment condition is seen in Fig. 15a where clustered slip was suppressed at grain boundaries and was induced near the grain boundary region of the adjacent grains. It is important to note that these slip systems have large misorientations with respect to those in the adjacent grains. In the modified heat treatment condition, Fig. 14c, clustered

slip was coincident across the grain boundaries and appears to have passed through the boundary and propagated into the adjacent grains without any appreciable misorientation. Furthermore, the relatively clean grain boundaries appeared to exert a minimal effect on the propagation of the slip in comparison with the conventional heat treatment condition. These observations indicate that the flow stress may be higher for the conventional treatment although the effect may not be large (28). In the material given the conventional heat treatment, strain cannot be as easily accommodated by deformation throughout the sample which can result in increased flow stresses near the region of the crack tip and higher crack growth rates. The improvement in the FCP performance at 427 deg C, then, was considered to primarily result from the alteration of the normally heterogeneous slip processes to homogeneous processes by the coarsening of γ'' particles during the modified treatment. Of secondary significance to the improved performance was the effect of the relatively clean grain boundaries on dislocation generation and reduced flow stress in the modified heat treatment condition.

In contrast to the 427 deg C behavior, the modified heat treatment produced slightly higher crack growth rates and an intergranular failure mode at 593 deg C in the Heat A material. This observation of intergranular failure for the modified heat treatment condition and the mixed mode failure for the conventional heat treatment condition at 593 deg C suggests that the air environment may have had a significant effect on the deformation mode. At this temperature oxidation can take place by diffusion at the crack tip, on grain boundaries, or preferentially on active slip planes resulting in intergranular or a mixture of transgranular and intergranular failure.

Previous work (29) has shown that air environments accelerate slip band development and increase transgranular crack propagation rates in Alloy X-750 when compared to vacuum. As shown in Fig. 14d, deformation in vacuum produced slip accumulation at grain boundaries which, in turn, produced the tendency for intergranular failure. The air environment at 593 deg C produced accelerated slip band formation and higher fatigue crack growth rates for both material conditions in air. However, the fracture surfaces indicated that, for the conventional treatment, the large grains fractured transgranularly and, where these slip planes intercept grain boundaries in adjacent grains, intergranular failure was observed at 593 deg C, Fig. 15b.

The modified treatment, in addition to enlarging the grain size, also altered the distribution and form of grain boundary Laves phase precipitates (11). Cracks can nucleate at precipitates or other grain boundary inclusions and propagate as a result of decreased fracture energy at the precipitate/matrix interface. From the examination of the deformation specimens, it was evident that the Laves phase was quite susceptible to embrittlement by air since fractured Laves particles were only observed in those specimens tested in air at 593 deg C. Although the modified treatment reduced the absolute quantity of the Laves phase, the redistribution resulted in a finer and more continuous coverage of the grain boundaries by the precipitate phases. Therefore,

if a greater percentage of the grain boundary area contains Laves phase precipitates, the material may be more susceptible to environmental embrittlement and intergranular failure. Thus, the results show that the reduced FCP performance at 593 deg C for the Heat A material given the modified heat treatment was primarily the result of the environmental susceptibility of the altered distribution and size of grain boundary particles and the tendency for slip accumulation at the grain boundaries. Of secondary importance to the reduced FCP performance was the larger grain size which may have contributed to the embrittlement and intergranular fracture in the Heat A Alloy 718 given the modified heat treatment and tested at 593 deg C.

Significant differences were observed in the FCP resistance of Heats A and B in the present study, but James (6) has reported little difference between the fatigue crack propagation performance of the two heats of Alloy 718 in his study. Comparison of the present FCP results for Heat A with James' results indicates that the FCP resistance of the Heat A material is slightly inferior to the alloys studied by James for basically similar heat treatments and test temperatures. As expected, small differences in melting procedures, composition, and heat treatment can have an effect on the properties of the Heat A and B materials used in the present study. Hardness values, γ'' particle diameters and volume fractions were less for the Heat B material. Differences in the atomic ratios (16) of Al, Ti, and Cb produce no consistent explanation of the behavior since the compositions of the alloys are similar, except that Heat A is high in Co and Heat B is low in P and S which could lead to segregation effects. It is likely that the smaller precipitate size in the Heat B material can account for the reduced matrix strength, the increased propensity for heterogeneous slip, and the increased crack growth rates in the conventional heat treatment condition.

The modified heat treatment coarsens the precipitates and promotes homogeneous deformation which decreases crack growth rates. In contrast to the Heat A behavior, the modified heat treatment also improved FCP resistance of the Heat B material at 593 deg C. There may be several explantions of this response. The modified heat treatment is seen to have coarsened the γ'' precipitates appreciably while producing a much lower volume fraction, a condition conducive of homogeneous slip. If failure is related to the interaction of slip and the grain boundaries, this effect would be expected to be less for the Heat B material because of the homogeneous deformation. The fracture surfaces for the Heat B material given the modified heat treatment and tested at 593 deg C exhibit a mixture of transgranular and intergranular modes of crack propagation which do not suggest the degree of embrittlement seen for the Heat A material. In addition, the susceptibility to the environmental effects of oxygen may have been reduced for the Heat B material either by the composition of the grain boundaries (low P and S) or by the nature of the grain boundary interfaces in this material. These effects will be explored in more detail in forthcoming studies of Alloy 718 (20).

CONCLUSIONS

The relationships between deformation, miocrostructure, and fatigue crack propagation behavior of Alloy 718 tested in air at 427 and 593 deg C have been studied. The following conclusions are drawn from the results:

1. The FCP resistance of Alloy 718 is significantly improved by the modified heat treatment in comparison to the conventional heat treatment properties. An exception occurs at 593 deg C for the Heat A material in which the FCP resistance was slightly reduced by the modified heat treatment.

2. The improved fatigue crack propagation resistance produced by the modified heat treatment is related to the basic deformation mechanism of Alloy 718. The effect of the modified heat treatment is to increase the γ'' particle size and decrease the γ'' density which favors homogeneous slip by matrix deformation and dislocations bypass of the γ'' particles.

3. Failure modes were transgranular for both the conventional and modified heat treatment conditions at the 427 deg C test temperatures. Although mixed or intergranular fracture paths were observed at 593 deg C the modified treatment increased the occurrence of intergranular fracture.

4. Environmental factors appeared to be significant at 593 deg C and severe embrittlement was evident for the Heat A specimens given the modified treatment. The reduction in FCP resistance for this condition may have been a result of the change in elemental distribution and grain boundary coverage produced by the modified heat treatment resulting in increased environmental sensitivity of the alloy to intergranular failure.

5. The FCP performance of the Heat A alloy was generally superior to that of Heat B alloy indicating that the effects of composition, melting, and processing methods require additional study in order that the properties of Alloy 718 may be fully optimized.

ACKNOWLEDGMENTS

We wish to thank J. T. Atwell for his assistance with the electron microscopy and T. R. Harrison for his assistance with the metallographic study. This work was supported by the Office of Naval Research and the U. S. Department of Energy.

REFERENCES

1. D. D. Keiser, "Heat Treat Cracking in Inconel 718, Its Cause and Prevention," ANC Tech. Report No. 606, Idaho National Engineering Laboratory, Idaho Falls, ID, 1975.

2. E. G. Thompson, S. Nunez, and M. Prager, "Practical Solutions to Strain-Age Cracking of Rene' 41," Welding Journal Welding Research Supplement, Vol. 47(7), 1968, pp. 299s-313s.

3. A. W. Dix and W. F. Savage, "Factors Influencing Strain Age Cracking in Inconel X-750," Welding Journal Welding Research Supplement, Vol. 50(6), 1971, 247s-252s.

4. J. R. Hawthorne, private communication, 1978.

5. K.Sadananda and P. Shahinian, "Effect of Heat Treatment on High Temperature Crack Growth Under Static Load in Alloy 718," NRL Memorandum Report 3727, Naval Research Laboratory, Washington, DC, 1978.

6. L. A. James, "Fatigue Crack Propagation Behavior in Inconel 718," Report HEDL-TME 75-80 Westinghouse Hanford Co., Richland, WA, September 1975.

7. L. A. James, "Fatigue Crack Growth in Inconel 718 Weldments at Elevated Temperatures," Welding Journal Welding Research Supplement, Vol. 57(1), 1978, pp. 17s-23s.

8. P. C. Paris and F. Erdogan, "A Critical Analysis of Crack Propagation Laws," Journal of Basic Engineering, Trans. ASME,Vol. 85(D), 1963, p. 528.

9. E.H. Niccolls, "A Correlation for Fatigue Crach Growth Rate," Scripta Met., Vol. 10, 1976, pp. 295-298.

10. J. Baïson, J. Masounave, and C. Bathias, "On the Relationship Between the Parameters of Paris' Law for Fatigue Crack Growth in Aluminium Alloys," Scripta Met., Vol. 11, 1977, pp. 1101-1106.

11. G. R. Evers, H. H. Smith, and D. J. Michel, "An Investigation of Second Phases in Alloy 718 Using Electrolytic Extraction Techniques," Metallography, Vol. 10, 1978, pp. 355-371.

12. G. T. Hahn and A. R. Rosenfield, "Metallurgical Factors Affecting Fracture Toughness of AluminumAlloys," Met. Trans., Vol. 6A, 1975, pp 653-668.

13. H. G. Popp and A. Coles, "Subcritical Crack Growth Criteria for Inconel 718 at Elevated Temperatures," Proceedings, Air Force Conference on Fatigue and Fracture of Aircraft Structures and Materials, H. A. Wood, et al. (Ed), AFFDL TR70144, Air Force Flight Dynamics Lab., 1970, p. 71-97.

14. H. L. Eiselstein, "Metallurgy of a Columbium-Hardened Nickel-Chromium-Iron-Alloy," Advances in the Technology of Stainless Steels and Related Alloys, ASTM STP 369, American Society for Testing and Materials, Philadelphia, Pa., 1965, pp. 62-79.

15. D. F. Pulonis, J. M. Oblak, and D. S. Duvall, "Precipitation in Nickel-Base Alloy718," Trans. ASM, 1969, Vol. 62, pp. 611-622.

16. R. Cozar and A. Pineau, "Morphology of γ ' and γ " Precipitates and Thermal Stability of Inconel 718 Type Alloys," Met. Trans., Vol. 4, 1973, p. 47.

17. R. S. Cremisio, H. M. Butler, and J. F. Radavich, "The Effect of Thermomechanical History on the Stability of Alloy 718," Journal of Metals, 1969, Vol. 21, No. 11, pp. 55-61.

18. J. F. Barker, E. W. Ross, and J. F. Radavich, "Long Time Stability of Inconel 718," Journal of Metals, 1970, Vol. 22, pp. 31-41.

19. W. J. Boesch and H. B. Canada, "Precipitation Reactions and Stability of Ni_3Cb in Inconel Alloy 718," Journal of Metals, 1969, Vol. 21, pp. 34-38.

20. H. H. Smith and D. J. Michel, "Effect of Microstructure on Deformation Behavior in Nickel-Base Alloys," to be submitted for publication, 1978.

21. B. Tomkins and W. D. Biggs, "Low Endurance Fatigue in Metals and Polymers," Journal of Material Science, Vol. 4, 1969, p. 544.

22. C. Laird, "Influence of Metallurgical Structure on the Mechanisms of Fatigue Crack Propagation," ASTM STP 415, American Society for Testing and Materials, Philadelphia, Pa., 1967, p. 131.

23. C. Laird amd R. De La Veaux, "Additional Evidence for the Plastic Blunting Process of Fatigue Crack Propagation," Met. Trans. A, Vol. 8A, 1977, pp. 657-664.

24. H. T. Michels and S. Floreen, "The Relationship Between Microstructure, Deformation Behavior, and Stress Corrosion Cracking Resistance of an Age-Hardened Ni-Base Alloy," Met. Trans., 1977, Vol. 8A, pp. 617-620.

25. A. W. Thompson and I. M. Bernstein, "The Role of Metallurgical Variables in Stress Corrosion Cracking and Hydrogen Embrittlement," Rockwell, International Science Center, 1975, SC-pp-75-63.

26. D. Fournier and A. Pineau, "Low Cycle Fatigue Behavior of Inconel 718 at 298K and 823K," Met. Trans. A, Vol. 8A, 1977, p. 1095.

27. B. H. Kerr, "The Influence of Ordering on the Engineering Properties of Two Phase Alloys - Part I: Mechanical Properties of γ' Precipitation Hardened Nickel-Base Superalloys," Order-Disorder Transformations in Alloys, H. Warlimont (ed.), Springer-Verlag, New York, 1974.

28. S. Miura and Y. Saeki, "Plastic Deformation of Aluminum Bicrystals <100> Oriented," Acta Metallurgica, Vol. 26, 1978, pp. 93-101.

29. H. H. Smith and P. Shahinian, "Influence of An Oxygen Atmosphere on Surface Slip in Fatigue of Inconel X-750 at 500 deg C," ASM Transactions, Vol. 62, 1969, p. 549-551.